



Thermodynamic modeling of binary CH₄–CO₂ fluid inclusions

Shide Mao ^{a,*}, Lanlan Shi ^b, Qiongbin Peng ^a, Mengxin Lü ^a

^a State Key Laboratory of Geological Processes and Mineral Resources, and School of Earth Sciences and Resources, China University of Geosciences, Beijing, 100083, China

^b Bayerisches Geoinstitut Universität Bayreuth, D-95440, Bayreuth, Germany



ARTICLE INFO

Article history:

Received 8 September 2015

Received in revised form

4 December 2015

Accepted 9 December 2015

Available online 12 December 2015

Keywords:

CH₄–CO₂

Equation of state

PVTx

Phase equilibria

Fluid inclusion

ABSTRACT

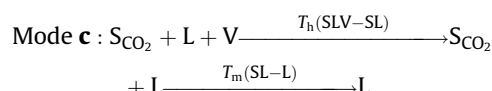
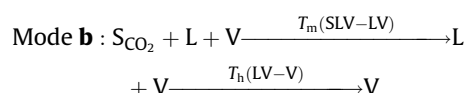
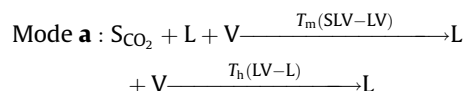
An equation of state (EOS) explicit in Helmholtz free energy has been improved to calculate the PVTx and vapor–liquid phase equilibrium properties of CH₄–CO₂ fluid mixture. This EOS, where four mixing parameters are used, is based on highly accurate EOSs recommended by NIST for pure components (CH₄ and CO₂) and contains a simple generalized departure function presented by Lemmon and Jacobsen (1999). Comparison with experimental data available indicates that the EOS can calculate both vapor–liquid phase equilibrium and volumetric properties of this binary fluid system with accuracy close to that of experimental data up to high temperature and pressure within full range of composition. The EOS of CH₄–CO₂ fluid, together with the updated Gibbs free energy model of solid CO₂ (dry ice), is applied to calculate the CH₄ content (x_{CH_4}) and molar volume (V_m) of the CH₄–CO₂ fluid inclusion based on the assumption that the volume of an inclusion keeps constant during heating and cooling. $V_m - x_{\text{CH}_4}$ diagrams are presented, which describe phase transitions involving vapor, liquid and CO₂ solid phases of CH₄–CO₂ fluid inclusions. Isochores of CH₄–CO₂ inclusions at given x_{CH_4} and V_m can be easily calculated from the improved EOS.

© 2015 Elsevier Ltd. All rights reserved.

1. Introduction

It is well-known that aqueous CO₂-bearing fluid inclusions are frequently found in hydrothermal ore deposits (Bodnar, 1995; Deng et al., 2015, 2014a; 2014b; Roedder and Bodnar, 1997; Yoo et al., 2011) and that CH₄-rich fluid inclusions are often found in sedimentary basins (Liu et al., 2009; Wang et al., 2007). However, water-free fluid inclusions that are approximated by the CH₄–CO₂ system are common in some metamorphic terranes (Beeskow et al., 2005; Cuney et al., 2007; Frey et al., 1980; Parry and Blamey, 2010; Roedder, 1984). Although complex phase behaviors of the CH₄–CO₂ system have been observed at low temperatures (van den Kerkhof, 1990), the CH₄–CO₂ inclusions often show three phases: solid CO₂ (S_{CO₂}) called dry ice, liquid (L) and vapor (V). Two phase-transition temperatures can be measured during heating from very low temperatures: the final melting temperature of solid CO₂ (T_m), and the V–L homogenization temperature (T_h) by the disappearance of liquid phase or vapor bubble. In the fluid inclusion studies, there are three kind of homogenization modes commonly observed in

terms of the disappearance sequence of phases:



For the homogenization modes **a** and **b**, $T_h > T_m$, but $T_h < T_m$ is for the homogenization mode **c**. The compositions, molar volumes and isochores of CH₄–CO₂ fluid inclusions can be obtained if the two phase-transition temperatures (T_h and T_m), which can be directly determined from the experimental microthermometric analysis, are combined with thermodynamic equation of state (EOS) because the volume and bulk composition of an inclusion keep constant during heating and cooling.

* Corresponding author.

E-mail address: maoshide@163.com (S. Mao).

In the past decades, some researchers devoted to the thermodynamic modeling of CH₄–CO₂ fluid inclusions (Herskowitz and Kisch, 1984; Heyen et al., 1982; Thiery and Dubessy, 1996; Thiery et al., 1994a, 1994b; van den Kerkhof, 1990). Heyen et al. (1982) simulated the fluid phase equilibria in CH₄–CO₂ system below 50 °C and 100 bar. Herskowitz and Kisch (1984) presented an algorithm to find compositions, molar volumes and isochores of CH₄–CO₂ fluid inclusions from T_h and T_m , where $T_h < T_m$ and a modified Redlich-Kwong EOS was used. Because cubic EOSs are poor in predicting the PVTx properties of fluids, Thiery et al. (1994a, 1994b) and Thiery and Dubessy (1996) modeled the phase equilibria of CH₄–CO₂ system including liquid, vapor and solid by the Soave-Redlich-Kwong EOS (Soave, 1972) and the PVTx properties by the Lee–Kesler correlation (Lee and Kesler, 1975) and applied them to the CH₄–CO₂ inclusions with $T_h > T_m$. At the end of last century, Lemmon and Jacobsen (1999) established a generalized EOS explicit in Helmholtz free energy to calculate thermodynamic properties of mixtures including CH₄ and CO₂ close to the estimated accuracy of experimental data. Their model contains two mixing parameters and a simple generalized departure function, and EOSs of pure fluids (Setzmann and Wagner, 1991; Span and Wagner, 1996) are from those that National Institute of Standards and Technology (NIST) recommends. However, the calculated saturated pressures in the near-critical region are much higher than experimental data at high temperatures, as can be seen later. Therefore, it is not satisfactorily solved how to model the thermodynamic properties of CH₄–CO₂ inclusions up to high temperatures and high pressures from a single EOS with experimental phase-transition temperatures T_h and T_m .

In this work, the generalized EOS of Lemmon and Jacobsen (1999) is improved by using four mixing parameters to predict the PVTx and vapor–liquid phase equilibrium properties of CH₄–CO₂ fluid firstly. Then the EOS of CH₄–CO₂ fluid, together with the updated Gibbs free energy mode of CO₂ solid of Jager and Span (2012), is applied to calculating the CH₄ content (x_{CH_4}) and molar volume (V_m) of CH₄–CO₂ fluid inclusions based on experimental T_h and/or T_m , and some V_m – x_{CH_4} diagrams are presented. Finally, isochores calculated from the improved EOS at given x_{CH_4} and V_m are made for CH₄–CO₂ inclusions.

2. Equation of state of CH₄–CO₂ fluid mixture

The EOS of CH₄–CO₂ fluid mixture is defined in terms of dimensionless Helmholtz free energy α as

$$\alpha = \frac{A}{RT} \quad (1)$$

where A is molar Helmholtz free energy, R is molar gas constant (8.314472 J mol⁻¹ K⁻¹), and T is temperature in K.

The dimensionless Helmholtz free energy α of the mixture is represented by

$$\alpha = \alpha_m^{\text{id}} + \alpha^E \quad (2)$$

where α_m^{id} is the dimensionless Helmholtz free energy of an ideal mixture and α^E is the excess dimensionless Helmholtz free energy. α_m^{id} comes directly from the fundamental equations of pure fluids and can be written as

$$\begin{aligned} \alpha_m^{\text{id}} &= \alpha_m^0(\delta, \tau, x) + \sum_{i=1}^2 x_i \alpha_i^r(\delta, \tau) \\ &= \sum_{i=1}^2 x_i [\alpha_i^0(\delta, \tau) + \ln(x_i)] + \sum_{i=1}^2 x_i \alpha_i^r(\delta, \tau) \end{aligned} \quad (3)$$

where α_m^0 is the ideal-gas part of dimensionless Helmholtz free energy of the mixture, α_i^0 and α_i^r are the ideal-gas part and residual part of dimensionless Helmholtz free energy of component i , respectively, x_i is the mole fraction of the component i . The superscripts “id”, “0” and “r” denote ideal mixing, the ideal-gas part and residual part of dimensionless Helmholtz free energy, respectively. The subscripts “i” and “m” denote the component and mixture, respectively. Here subscripts 1 and 2 refer to CH₄ and CO₂, respectively, so does the following equations. δ and τ are reduced parameters, which are defined by

$$\delta = \frac{\rho}{\rho_c} \quad (4)$$

$$\tau = \frac{T_c}{T} \quad (5)$$

where ρ is the density of mixture, and ρ_c and T_c are defined as

$$\rho_c = \left[\sum_{i=1}^2 \frac{x_i}{\rho_{ci}} + x_1 x_2 \zeta_{12} \right]^{-1} \quad (6)$$

$$T_c = \sum_{i=1}^2 x_i T_{ci} + x_1^{\beta_{12}} x_2 \varsigma_{12} \quad (7)$$

where ρ_{ci} and T_{ci} are the critical density and critical temperature of the component i , respectively, x_1 and x_2 denote mole fraction of components 1 and 2, and ζ_{12} , ς_{12} , and β_{12} are the mixture-dependent binary parameters associated with components 1 and 2 (CH₄ and CO₂).

The α^E in Eq. (2) is given by

$$\alpha^E = x_1 x_2 F_{12} \sum_{k=1}^{10} N_k \delta^{d_k} \tau^{t_k} \quad (8)$$

where N_k , d_k and t_k are general parameters independent of fluids, which can be found from the model of Lemmon and Jacobsen (1999) (Table 1), F_{12} is a binary parameter of components 1 and 2.

The residual part of dimensionless Helmholtz free energy of CH₄–CO₂ fluid mixture α^r is defined by

$$\alpha^r = \sum_{i=1}^2 x_i \alpha_i^r(\delta, \tau) + \alpha^E(\delta, \tau, x) \quad (9)$$

Here EOSs of pure CH₄ and CO₂ fluids are from the references (Setzmann and Wagner, 1991; Span and Wagner, 1996). These EOSs are all explicit in dimensionless Helmholtz energy and are considered to be the most accurate equations for thermodynamic properties of the two pure fluids. Critical parameters of the pure

Table 1
Coefficients and exponents of Eq. (8).

k	N_k	d_k	t_k
1	-2.45476271425D-2	1	2
2	-2.41206117483D-1	1	4
3	-5.13801950309D-3	1	-2
4	-2.39824834123D-2	2	1
5	2.59772344008D-1	3	4
6	-1.72014123104D-1	4	4
7	4.29490028551D-2	5	4
8	-2.02108593862D-4	6	0
9	-3.82984234857D-3	6	4
10	2.69923313540D-6	8	-2

CH_4 and CO_2 are listed in Table 2.

Values of the binary parameters (ζ_{12} , ς_{12} , β_{12} and F_{12}) in above equations for the $\text{CH}_4\text{--CO}_2$ fluid mixture are determined by a non-linear regression to experimental $PVTx$ data (Arai et al., 1971; Brugge et al., 1989; Hwang et al., 1976; Magee and Ely, 1988; Mondejar et al., 2012; Seitz and Blencoe, 1996; Seitz et al., 1996; Tong and Liu, 1984) and the vapor–liquid phase equilibrium data (Al-Sahhaf et al., 1983; Bian et al., 1993; Davalos et al., 1976; Donnelly and Katz, 1954; Hwang et al., 1976; Joffe, 1976; Mraw et al., 1978; Neumann and Walch, 1968; Somait and Kidnay, 1978; Vrabec and Fischer, 1996; Webster and Kidnay, 2001; Wei et al., 1995; Xu et al., 1992). In the fitting, objective function is defined as the sum of relative deviation of density and fugacity difference of each component between vapor and liquid phases. Regressed parameters are listed in Table 3.

The density or molar volume of the $\text{CH}_4\text{--CO}_2$ mixture can be calculated from Eq. (10) with the Newton iterative method.

$$P = \rho RT [1 + \delta\alpha_\delta^r] \quad (10)$$

where P is pressure, and $\delta\alpha_\delta^r$ is the derivative of α^r with respect to δ . If the mixture is in vapor or supercritical state, the initial density of mixture can be set equal to that of ideal gas. If the mixture is in liquid state, the initial density can be set as the saturated liquid density of pure CO_2 at temperature above 216.592 K, below which the saturated liquid density of pure CH_4 can be set as the initial density. The average absolute density deviation of this EOS from all experimental $PVTx$ data is 0.40%, better than that of previous EOS used by Lemmon and Jacobsen (1999), which is about 0.50%. Fig. 1 shows deviations of calculated densities from experimental densities (Brugge et al., 1989; Magee and Ely, 1988; Mondejar et al., 2012; Seitz and Blencoe, 1996) up to 673 K and 1000 bar, which is general below 1%, close to or within experimental uncertainties.

Fugacity and fugacity coefficient of the component i (CH_4 or CO_2) can be calculated from the following equations:

$$f_i = x_i \rho RT \exp\left(\frac{\partial n\alpha^r}{\partial n_i}\right)_{T,V,n_j} \quad (11)$$

$$\ln \varphi_i = \left(\frac{\partial n\alpha^r}{\partial n_i}\right)_{T,V,n_j} - \ln(1 + \delta\alpha_\delta^r) \quad (12)$$

$$\left(\frac{\partial n\alpha^r}{\partial n_i}\right)_{T,V,n_j} = \alpha^r + n \left(\frac{\partial \alpha^r}{\partial n_i}\right)_{T,V,n_j} \quad (13)$$

$$\begin{aligned} n \left(\frac{\partial \alpha^r}{\partial n_i}\right)_{T,V,n_j} &= \delta\alpha_\delta^r \left[1 - \frac{1}{\rho_c} \left[\left(\frac{\partial \rho_c}{\partial x_i}\right)_{x_j} - \sum_{k=1}^2 x_k \left(\frac{\partial \rho_c}{\partial x_k}\right)_{x_j} \right] \right] \\ &\quad + \tau\alpha_\tau^r \frac{1}{T_c} \left[\left(\frac{\partial T_c}{\partial x_i}\right)_{x_j} - \sum_{k=1}^2 x_k \left(\frac{\partial T_c}{\partial x_k}\right)_{x_j} \right] + \alpha_{x_i}^r \\ &\quad - \sum_{k=1}^2 x_k \alpha_{x_k}^r \end{aligned} \quad (14)$$

where f_i is the fugacity of component CH_4 or CO_2 , n is the total mole numbers, V is the total volume, n_i is the mole number of component

i , n_j is the mole number of component j and signifies that all mole numbers are held constant except n_i , φ_i is the fugacity coefficient of component i , and α^r , $\alpha_{x_i}^r$ and $\alpha_{x_k}^r$ are the derivatives of α^r with respect to τ , x_i and x_k , respectively.

Vapor–liquid phase equilibrium compositions and densities at a given temperature (T) and pressure (P) can be calculated by the iterative algorithm of Michelsen (1993) as used by our previous study for the $\text{NH}_3\text{--H}_2\text{O}$ system (Mao et al., 2015). Assume that the total mole number of $\text{CH}_4\text{--CO}_2$ mixture is 1, bulk composition of component i is M_i , mole number of vapor phase is N^V , and vapor and liquid compositions of component i are x_i and y_i , then x_i and y_i at a given T and P can be calculated from the following steps:

Step 1: Give a group of initial reasonable guess values (between 0 and 1) for M_i , x_i and y_i .

Step 2: First calculate the vapor and liquid densities form Eq. (10), then calculate the fugacity coefficient of component i in vapor phase (φ_i^V) and liquid phase (φ_i^L) from Eq. (12).

Step 3: Define an equilibrium factor $k_i = y_i/x_i = \varphi_i^L/\varphi_i^V$, then calculate k_i from φ_i^V and φ_i^L .

Step 4: Calculate N^V from the normalized equation $\sum_{i=1}^2 M_i(k_i - 1)/(1 - N^V + N^V k_i) = 0$.

Step 5: Calculate x_i and y_i from equations $x_i = M_i/(1 - N^V + N^V k_i)$ and $y_i = k_i M_i/(1 - N^V + N^V k_i)$, respectively.

Step 6: Go to Step 2, and recalculate φ_i^V , φ_i^L , k_i , N^V , x_i and y_i in turn until the calculated N^V keeps unchangeable. Then x_i and y_i are the vapor–liquid phase equilibrium compositions, and densities are the saturated densities. It should be noted that when T and P approach critical point, initial values for x_i and y_i lie in a narrow range, which are frequently set by experience.

Fig. 2 compares the vapor–liquid phase equilibrium curves calculated from this EOS with experimental data at different temperatures, where the calculated pressures from the two-parameter EOS of Lemmon and Jacobsen (1999) are also added for comparison. It can be seen that pressures as a function of composition at -43.15°C (230 K) calculated from this EOS and Lemmon and Jacobsen (1999) are both in good agreement with experimental data (Webster and Kidnay, 2001; Wei et al., 1995). The V-L equilibrium pressures calculated from this EOS at -3.15°C (270 K) are also in agreement with experimental data (Al-Sahhaf et al., 1983; Davalos et al., 1976; Webster and Kidnay, 2001), better than those calculated from the EOS of Lemmon and Jacobsen in the near-critical region.

3. Fugacity and molar volume of dry ice

In order to obtain compositions and molar volumes of $\text{CH}_4\text{--CO}_2$ fluid inclusions, fugacity and molar volume of solid CO_2 (dry ice) must be known, which is a function of T and P . Jager and Span (2012) established an EOS explicit in the Gibbs free energy for solid CO_2 (dry ice), and this EOS can be used to calculate the fugacity and molar volume of dry ice by the following thermodynamic relations:

$$RT \ln \frac{f_{\text{CO}_2}^s(T, P)}{f_{\text{CO}_2}^s(T, P_s)} = g_{\text{CO}_2}^s(T, P) - g_{\text{CO}_2}^s(T, P_s) \quad (15)$$

$$V_m^s(T, P) = \left(\frac{\partial g_{\text{CO}_2}^s(T, P)}{\partial P} \right)_T \quad (16)$$

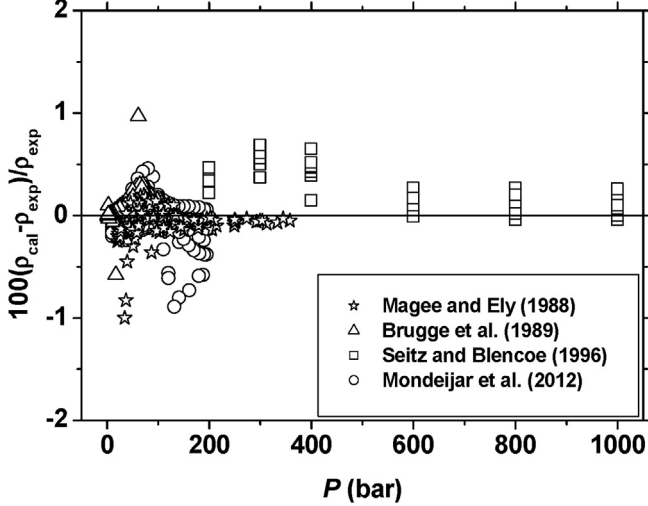
where $f_{\text{CO}_2}^s(T, P)$ is the fugacity of solid CO_2 at T and P , $f_{\text{CO}_2}^s(T, P_s)$ is the fugacity of solid CO_2 at T and P_s (the saturated pressure of pure

Table 2
Critical parameters of pure fluids.

i	$T_{ci}(\text{K})$	$\rho_{ci}(\text{mol dm}^{-3})$
CH_4	190.564	10.139342719
CO_2	304.1282	10.624978698

Table 3Parameters of the CH₄–CO₂ fluid mixture.

Mixture	F_{12}	$\zeta_{12}(\text{dm}^3 \text{ mol}^{-1})$	$\zeta_{12}(\text{K})$	β_{12}
CH ₄ –CO ₂	0.12844025D+01	0.35751245D−02	−0.43720344D+02	0.10358865D+01

Note: subscripts 1 and 2 refer to CH₄ and CO₂, respectively.**Fig. 1.** Calculated density deviations of the CH₄–CO₂ fluid mixture: ρ_{cal} is the calculated density from this work, ρ_{exp} is experimental density, and P is pressure.

CO₂ at solid-vapor equilibria, which is a function of T and can be calculated from the empirical equation in the reference (Span and Wagner, 1996)), $g_{\text{CO}_2}^s(T, P)$ is the molar Gibbs free energy of solid CO₂ at T and P , $g_{\text{CO}_2}^s(T, P_s)$ is the molar Gibbs free energy of solid CO₂ at T and P_s , and $V_m^s(T, P)$ is the molar volume of solid CO₂ at T and P . $f_{\text{CO}_2}^s(T, P_s)$ equals the fugacity of pure CO₂ vapor at T and P_s , which can be calculated from the EOS of fluid CO₂ (Span and Wagner, 1996). $g_{\text{CO}_2}^s$ is calculated from Jager and Span (2012) (Details see Appendix I). Once T and P are given, the fugacity and molar volume of solid CO₂ can be accurately obtained from Eqs. (15) and (16), respectively.

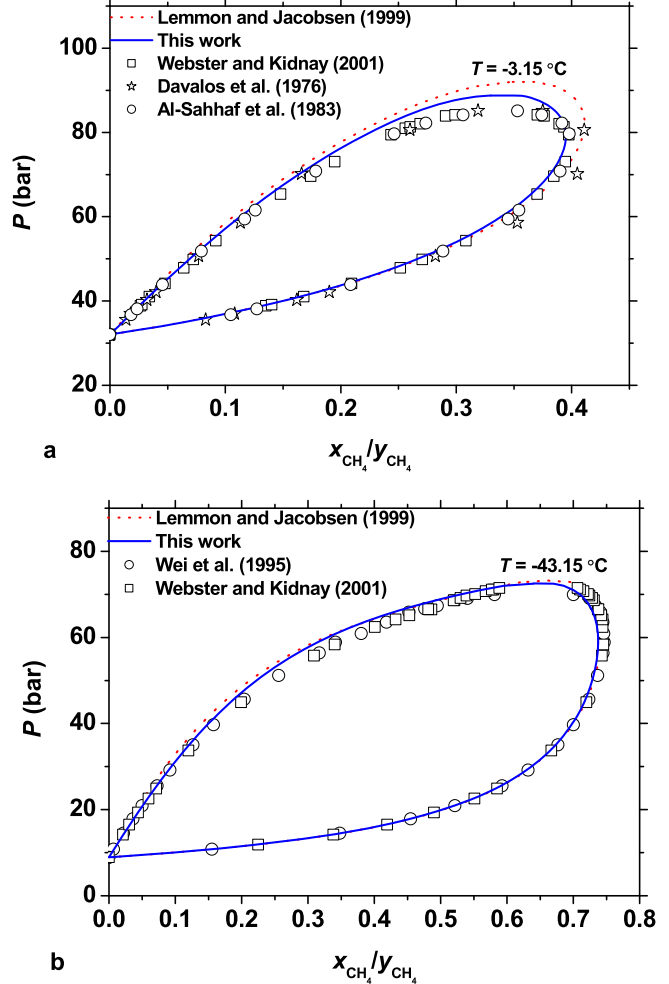
Fig. 3 shows the calculated P - T curve along the solid-liquid-vapor locus of CH₄–CO₂ system, which is in good agreement with the whole experimental data of Davis et al. (1962) and the high-temperature data of Donnelly and Katz (1954). This, from another aspect, proves the reliability of the used EOSs of both fluid and solid.

4. Application to CH₄–CO₂ fluid inclusions

4.1. Compositions and molar volumes of CH₄–CO₂ inclusions

There are two approaches to determine compositions and molar volumes of CH₄–CO₂ inclusions. **Method one** is using the estimated volume fraction of vapor bubble at $T_m(\text{SLV-LV})$ for the homogenization modes **a** and **b** or using the volume fraction of dry ice at $T_h(\text{SLV-SL})$ for the homogenization mode **c**. According to the Gibbs phase rule, the number of free degree is one for the three-phase binary system. Therefore, once $T_m(\text{SLV-LV})$ or $T_h(\text{SLV-SL})$ is determined by microthermometric analysis, the pressure, compositions and densities (or molar volumes) can be obtained from the EOSs aforementioned.

For the homogenization modes **a** and **b**, the following equations can calculate the compositions and molar volumes of CH₄–CO₂ inclusions:

**Fig. 2.** Vapor-liquid phase equilibria of the CH₄–CO₂ system at different temperatures: P is pressure, T is temperature, and x_{CH_4} and y_{CH_4} are mole fraction of CH₄ in liquid and vapor phase, respectively.

$$x_{\text{CH}_4}^{\text{bulk}} = \left(\frac{F_V y_{\text{CH}_4}}{V_m^V} + \frac{(1 - F_V)x_{\text{CH}_4}}{V_m^L} \right) \Big/ \left(\frac{F_V}{V_m^V} + \frac{1 - F_V}{V_m^L} \right) \quad (17)$$

$$V_m = \left(\frac{F_V}{V_m^V} + \frac{1 - F_V}{V_m^L} \right)^{-1} \quad (18)$$

where $x_{\text{CH}_4}^{\text{bulk}}$ is the mole fraction of CH₄ in the total inclusion, F_V is the estimated volume fraction of vapor bubble at $T_m(\text{SLV-LV})$, y_{CH_4} is the mole fraction of CH₄ in vapor phase, x_{CH_4} is the mole fraction of CH₄ in liquid phase, V_m^V , V_m^L and V_m denote the molar volume of vapor phase, liquid phase and the total inclusion, respectively. When $T_m(\text{SLV-LV})$ is measured, the pressure can be acquired by a bisection algorithm: First give an initial $P (>P_s)$, and calculate the vapor–liquid equilibrium compositions, densities, component

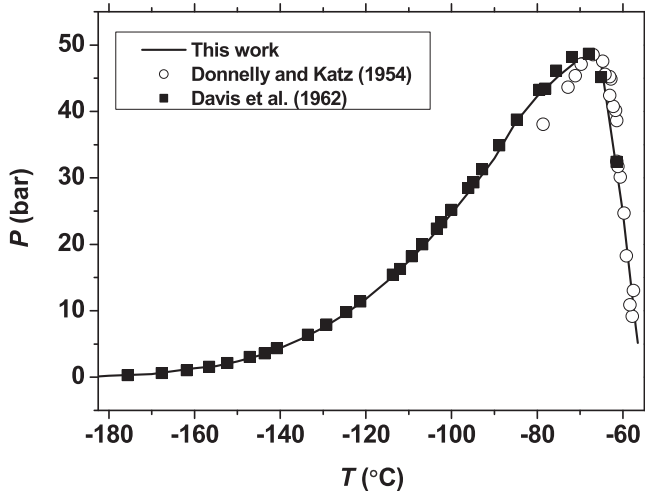


Fig. 3. Temperature-pressure relation along the solid-liquid-vapor locus of $\text{CH}_4\text{-CO}_2$ system: P is pressure and T is temperature.

fugacity in each fluid phase by $T_m(\text{SLV-LV})$ and $(P + P_s)/2$ by the iterative method of Michelisen (1993), then compare the fugacity of CO_2 in vapor phase to that of dry ice calculated from Eq. (15). If the

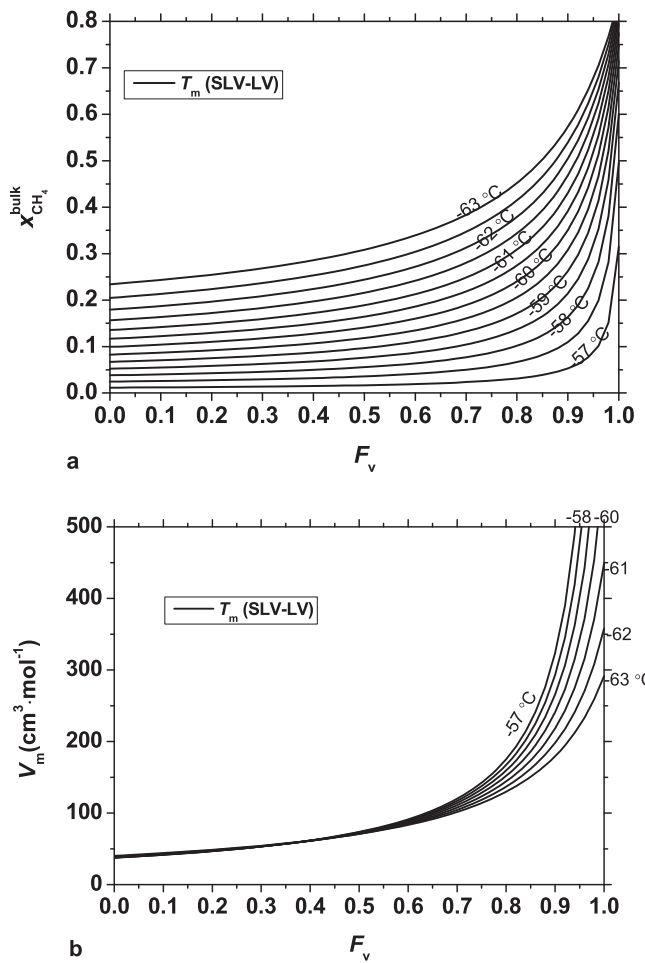


Fig. 4. Calculated compositions and molar volumes of $\text{CH}_4\text{-CO}_2$ inclusions by the volume fractions of vapor bubble and the melting temperatures of dry ice: $x_{\text{CH}_4}^{\text{bulk}}$ is the mole fraction of CH_4 in the total inclusion, $T_m(\text{SLV-LV})$ is the melting temperature of dry ice coexisting with liquid and vapor, V_m is the molar volume of fluid inclusion, and F_v is the volume fraction of vapor bubble at $T_m(\text{SLV-LV})$.

fugacity of CO_2 in vapor phase is greater than that of dry ice, then increase P . Otherwise, decreasing P until the calculated fugacity of CO_2 in vapor phase equal to that of dry ice. Under this condition, x_{CH_4} , y_{CH_4} , V_m^V and V_m^L are the phase-equilibrium compositions and saturated molar volumes.

For the homogenization mode **c**, the following equations can calculate the compositions and molar volumes of $\text{CH}_4\text{-CO}_2$ inclusions:

$$x_{\text{CH}_4}^{\text{bulk}} = \left(\frac{(1 - F_s)x_{\text{CH}_4}}{V_m^L} \right) \Big/ \left(\frac{F_s}{V_m^S} + \frac{1 - F_s}{V_m^L} \right) \quad (19)$$

$$V_m = \left(\frac{F_s}{V_m^S} + \frac{1 - F_s}{V_m^L} \right)^{-1} \quad (20)$$

where F_s is the volume fraction of dry ice at $T_h(\text{SLV-SL})$. The calculation approach is similar to that used in the homogenization modes **a** and **b**.

The calculated compositions and molar volumes of $\text{CH}_4\text{-CO}_2$ inclusions by $T_m(\text{SLV-LV})$ and F_v are shown in Fig. 4, from which it can be seen that $x_{\text{CH}_4}^{\text{bulk}}$ and V_m increase with the increase of F_v at the

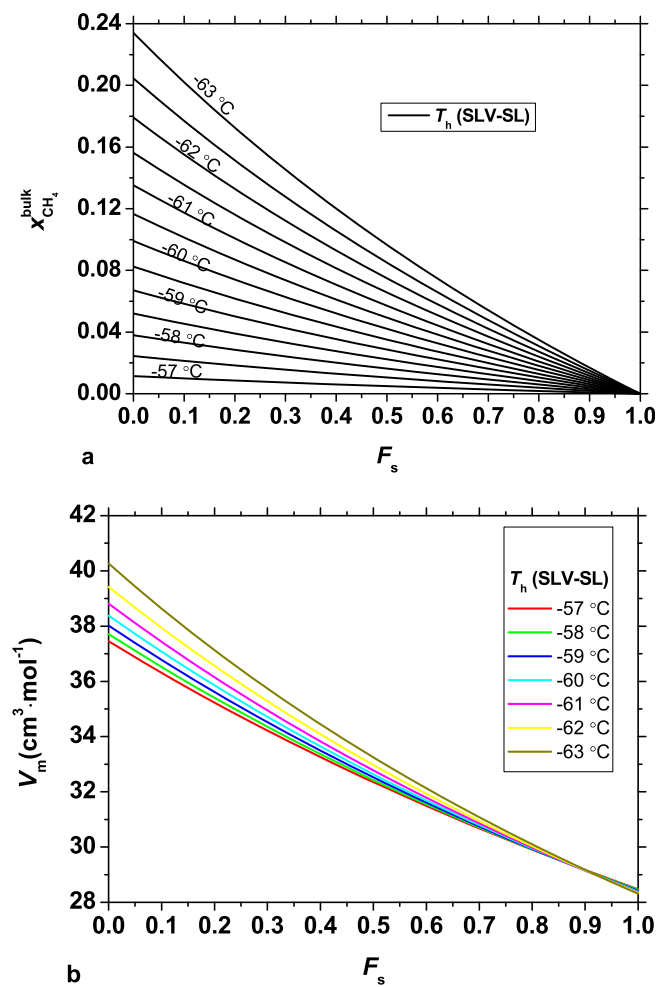


Fig. 5. Calculated compositions and molar volumes of $\text{CH}_4\text{-CO}_2$ inclusions by the volume fractions of dry ice and the partial homogenization temperatures: $x_{\text{CH}_4}^{\text{bulk}}$ is the mole fraction of CH_4 in the total inclusion, $T_h(\text{SLV-SL})$ is the partial homogenization temperature by the disappearance of vapor bubble, V_m is the molar volume of fluid inclusion, and F_s is the volume fraction of dry ice at $T_h(\text{SLV-SL})$.

same T_m (SLV-LV). But $x_{\text{CH}_4}^{\text{bulk}}$ decreases with increasing T_m (SLV-LV) at the same F_V , and V_m is on the contrary. The calculated compositions and molar volumes of CH_4-CO_2 inclusions by T_h (SLV-SL) and F_s are shown in Fig. 5, from which it can be seen that $x_{\text{CH}_4}^{\text{bulk}}$ and V_m decrease with the increase of F_s at the same T_h (SLV-SL), and almost decrease with the increasing T_h (SLV-SL) at the same F_s .

It should be noted that the visual estimation of F_V or F_s in fluid inclusions involve large errors, particularly for fluid inclusions of irregular shape. An improved method of Bakker and Diamond (2006) can be used to estimate volume fraction by the petrographic microscope in conjunction with a spindle-stage. The relative accuracy of the estimated volume fraction is $\pm 4\%$, much better than traditional estimation method which involves measuring area-fractions of the phases projected in the microscope and then making rough corrections for the third dimension. But this method is time-consuming and unfit for negative-crystal inclusions.

In order to overcome flaws in **Method one**, the two phase-transition temperatures T_m and T_h can be directly used to obtain

the compositions and molar volumes of CH_4-CO_2 inclusions by combining with the EOSs of CH_4-CO_2 fluid and dry ice. This approach is called **Method two**. For the homogenization modes **a** and **b**, calculated $V_m - x_{\text{CH}_4}$ diagrams are presented in Fig. 6, where the iso- T_m curves are calculated from Eqs. (17)–(18) by the F_V (between 0 and 1), and the iso- T_h curves are calculated from the improved EOS of CH_4-CO_2 fluid using the aforementioned iterative algorithm of Michelsen (1993). The intersection point of the iso- T_m (SLV-LV) and iso- T_h curves in Fig. 6 corresponds to the composition and molar volume of an inclusion. Fig. 6a and b denote that fluid inclusions homogenize to liquid phase and vapor phase, respectively. For the homogenization mode **c**, calculated $V_m - x_{\text{CH}_4}$ diagram is presented in Fig. 7, where the iso- T_h (SLV-SL) curves are calculated from Eqs. (19) and (20) by the F_s (between 0 and 1), and the iso- T_m (SL-L) curves are calculated by an iterative approach under the condition that the fugacity of dry ice equals to that of CO_2 in liquid phase. The intersection point of the iso- T_h (SLV-SL) and iso- T_m (SL-L) curves determines the composition and molar volume of an inclusion.

4.2. Isochore calculation of CH_4-CO_2 inclusions

Construction of isochores along which the trapped fluids in minerals evolve is the final goal to inclusion researchers. Experimental data for the iso- T_h or iso- T_m curves approximated as isochores are not reported for the CH_4-CO_2 system. Therefore, the predictive EOSs are the best choice to calculate the isochores of CH_4-CO_2 inclusions. Because this EOS is established on the basis of the Helmholtz energy with good extrapolated ability (Span and Wagner, 1997) and reproduce the molar volumes and densities within or close to experimental uncertainties, it can be used to calculate the isochores of CH_4-CO_2 inclusions. When the composition and molar volume of an inclusion are obtained from the two phase-transition temperatures (T_h and T_m), the pressure can be directly calculated from Eq. (10) at a given temperature. Fig. 8 shows the isochores of the two compositions calculated from the improved EOS, from which it can be seen that the isochores of CH_4-CO_2 inclusions are a bit curved and cannot be approximated as straight lines.

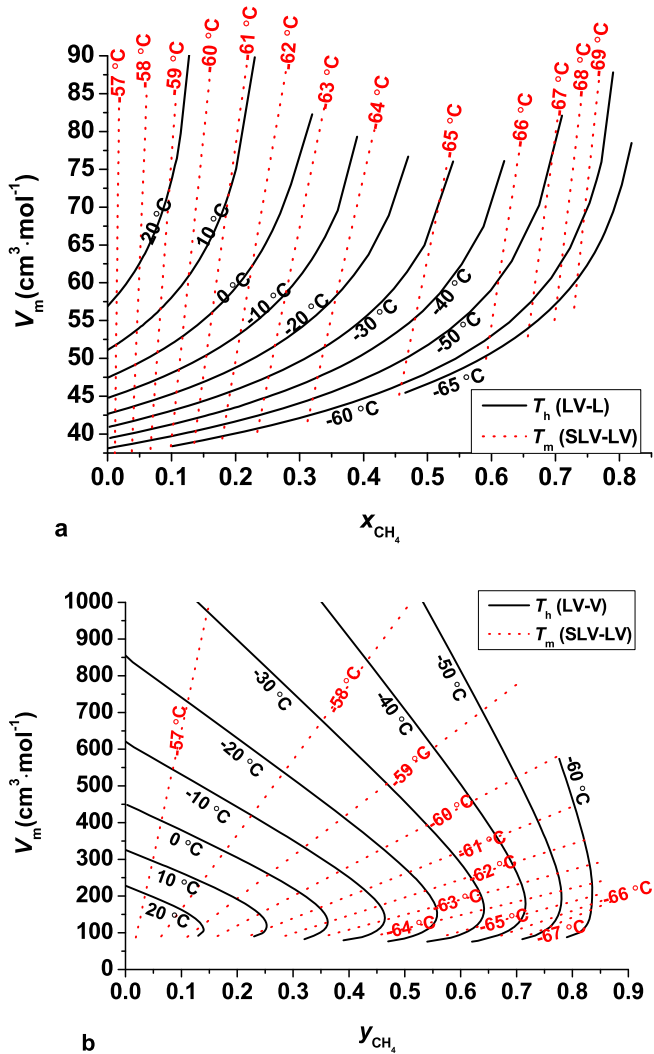


Fig. 6. Calculated compositions and molar volumes of CH_4-CO_2 inclusions by the phase-transition temperatures (T_m (SLV-LV) $<$ T_h (LV-L) or T_h (LV-V)): x_{CH_4} and y_{CH_4} are mole fraction of CH_4 in liquid and vapor phase, respectively, V_m is the molar volume of fluid inclusion, T_h (LV-L) is the total homogenization temperature by the disappearance of vapor bubble, T_h (LV-V) is the total homogenization temperature by the disappearance of liquid phase, and T_m (SLV-LV) is the melting temperature of dry ice coexisting with liquid and vapor.

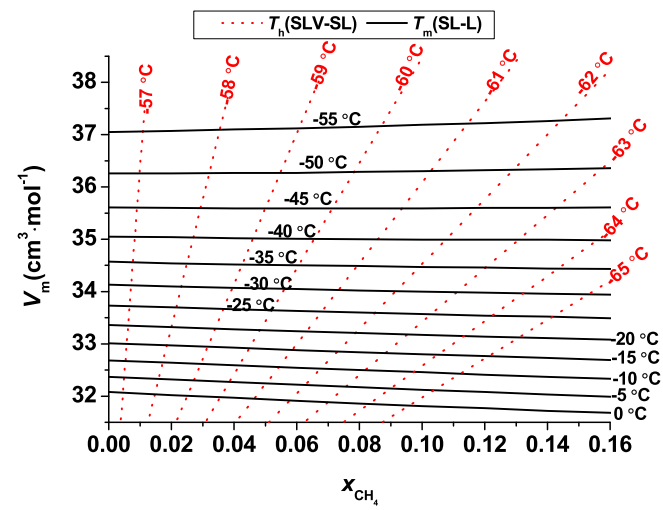


Fig. 7. Calculated compositions and molar volumes of CH_4-CO_2 inclusions by the phase-transition temperatures (T_h (SLV-SL) $<$ T_m (SL-L)): x_{CH_4} is mole fraction of CH_4 , V_m is the molar volume of fluid inclusion, T_h (SLV-SL) is the partial homogenization temperature by the disappearance of vapor bubble, and T_m (SL-L) is the total homogenization temperature by the disappearance of dry ice.

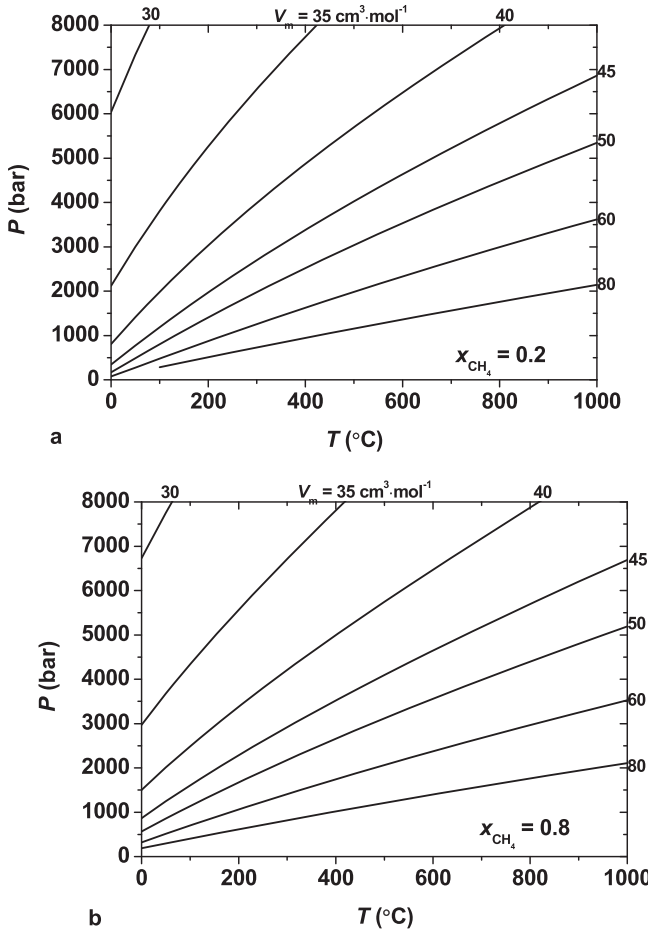


Fig. 8. Calculated isochores of the $\text{CH}_4\text{-CO}_2$ fluid system: T is temperature, P is pressure, and V_m is molar volume.

5. Conclusions

A fundamental EOS for the Helmholtz free energy of $\text{CH}_4\text{-CO}_2$ fluid mixtures has been improved by using four mixing parameters, from which the $PVTx$ and vapor–liquid equilibrium properties can be obtained by thermodynamic relations. The EOS can better reproduce the experimental volume and vapor–liquid phase equilibrium data available up to 623 K and 1000 bar, with or close to experimental accuracy.

The EOS of $\text{CH}_4\text{-CO}_2$ fluid, combined with the updated Gibbs free energy model of solid CO_2 , is applied to studies of $\text{CH}_4\text{-CO}_2$ fluid inclusions to determine the compositions and molar volumes from two-phase-transition temperatures T_h and T_m . The calculated $V_m - x_{\text{CH}_4}$ diagrams and the isochores of $\text{CH}_4\text{-CO}_2$ inclusions can be used to interpret the corresponding microthermometric and Raman analysis data of $\text{CH}_4\text{-CO}_2$ inclusions. It should be noted that experimental volumetric data at high temperatures and pressures (e.g., above 623 K and 1000 bar) are still lacking for the $\text{CH}_4\text{-CO}_2$ fluid mixtures, and future experimental studies of this system can be focused on this temperature-pressure region.

Acknowledgments

We thank three anonymous reviewers for their detailed and helpful comments, which improved greatly the quality of manuscript. This work is supported by the National Natural Science Foundation of China (41173072), the National Key Basic Research

Development Program (2015CB452606), and the Fundamental Research Funds for the Central Universities (2652013032).

Appendix I. The EOS of solid CO_2 (dry ice)

The EOS of solid CO_2 is from Jager and Span (2012), which is explicit in the Gibbs free energy $g_{\text{CO}_2}^s$ as follows:

$$\begin{aligned} \frac{g_{\text{CO}_2}^s}{RT_0} = & g_0 + g_1 \Delta \vartheta + g_2 \Delta \vartheta^2 \\ & + g_3 \left\{ \ln \left(\frac{\vartheta^2 + g_4^2}{1 + g_4^2} \right) - \frac{2\vartheta}{g_4} \left[\arctan \left(\frac{\vartheta}{g_4} \right) - \arctan \left(\frac{1}{g_4} \right) \right] \right\} \\ & + g_5 \left\{ \ln \left(\frac{\vartheta^2 + g_6^2}{1 + g_6^2} \right) - \frac{2\vartheta}{g_6} \left[\arctan \left(\frac{\vartheta}{g_6} \right) - \arctan \left(\frac{1}{g_6} \right) \right] \right\} \\ & + g_7 \Delta \pi \left[e^{f_\alpha(\vartheta)} + K(\vartheta) g_8 \right] \\ & + g_9 K(\vartheta) \left[(\pi + g_{10})^{(n-1)/n} - (1 + g_{10})^{(n-1)/n} \right] \end{aligned} \quad (\text{A1})$$

with

$$\begin{aligned} f_\alpha(\vartheta) = & g_0^\alpha (\vartheta^2 - 1) + g_1^\alpha \ln \left(\frac{\vartheta^2 - g_2^\alpha \vartheta + g_3^\alpha}{1 - g_2^\alpha + g_3^\alpha} \right) \\ & + g_4^\alpha \ln \left(\frac{\vartheta^2 + g_2^\alpha \vartheta + g_3^\alpha}{1 + g_2^\alpha + g_3^\alpha} \right) \\ & + g_5^\alpha \left[\arctan \left(\frac{\vartheta - g_6^\alpha}{g_7^\alpha} \right) - \arctan \left(\frac{1 - g_6^\alpha}{g_7^\alpha} \right) \right] \\ & + g_8^\alpha \left[\arctan \left(\frac{\vartheta + g_6^\alpha}{g_7^\alpha} \right) - \arctan \left(\frac{1 + g_6^\alpha}{g_7^\alpha} \right) \right] \end{aligned} \quad (\text{A2})$$

$$K(\vartheta) = g_0^\kappa \vartheta^2 + g_1^\kappa \vartheta + g_2^\kappa \quad (\text{A3})$$

where $R=8.314472 \text{ J} \cdot \text{mol}^{-1} \cdot \text{K}^{-1}$. The temperature T and the pressure P are replaced by the reduced temperature ϑ and the reduced pressure π . It is:

$$\vartheta = \frac{T}{T_0}, \quad \Delta \vartheta = \vartheta - 1, \quad \pi = \frac{P}{P_0}, \quad \Delta \pi = \pi - 1$$

where $T_0 = 150 \text{ K}$, and $P_0 = 101325 \text{ Pa}$. The parameters ($g_0\text{--}g_{10}$, $g_0^\alpha\text{--}g_8^\alpha$, $g_0^\kappa\text{--}g_2^\kappa$ and n) in Eqs. (A1) to (A3) are listed in Table A1.

Table A1
Values for the parameters of Eqs. (A1) to (A3)

$g_0 = -2.6385478 \times 10^0$	$g_0^\alpha = 3.9993365 \times 10^{-2}$
$g_1 = 4.5088732 \times 10^0$	$g_1^\alpha = 2.3945101 \times 10^{-3}$
$g_2 = -2.0109135 \times 10^0$	$g_2^\alpha = 3.2839467 \times 10^{-1}$
$g_3 = -2.7976237 \times 10^0$	$g_3^\alpha = 5.7918471 \times 10^{-2}$
$g_4 = 2.6427834 \times 10^{-1}$	$g_4^\alpha = 2.3945101 \times 10^{-3}$
$g_5 = 3.8259935 \times 10^0$	$g_5^\alpha = -2.6531689 \times 10^{-3}$
$g_6 = 3.1711996 \times 10^{-1}$	$g_6^\alpha = 1.6419734 \times 10^{-1}$
$g_7 = 2.2087195 \times 10^{-3}$	$g_7^\alpha = 1.7594802 \times 10^{-1}$
$g_8 = -1.1289668 \times 10^0$	$g_8^\alpha = 2.6531689 \times 10^{-3}$
$g_9 = 9.2923982 \times 10^{-3}$	$g_9^\alpha = 2.2690751 \times 10^{-1}$
$g_{10} = 3.3914617 \times 10^3$	$g_{10}^\alpha = -7.5019750 \times 10^{-2}$
$n = 7$	$g_2^\kappa = 2.6442913 \times 10^{-1}$

References

- Al-Sahaf, T.A., Kidnay, A.J., Sloan, E.D., 1983. Liquid + vapor equilibria in the $\text{N}_2+\text{CO}_2+\text{CH}_4$ system. *Ind. Eng. Chem. Fundam.* 22, 372–380.
- Arai, Y., Kaminishi, G.-I., Saito, S., 1971. The experimental determination of the PVTX relations for the carbon dioxide-nitrogen and the carbon dioxide-methane systems. *J. Chem. Eng. Jpn.* 4 (2), 113–122.
- Bakker, R.J., Diamond, L.W., 2006. Estimation of volume fractions of liquid and vapor phases in fluid inclusions, and definition of inclusion shapes. *Am. Mineral.* 91, 635–657.
- Beeskow, B., Rankin, A.H., Murphy, P.J., Treloar, P.J., 2005. Mixed CH_4-CO_2 fluid inclusions in quartz from the South Wales Coalfield as suitable natural calibration standards for microthermometry and Raman spectroscopy. *Chem. Geol.* 223 (1–3), 3–15.
- Bian, B., Wang, Y., Shi, J., Zhao, E., Lu, B.C.-Y., 1993. Simultaneous determination of vapor-liquid equilibrium and molar volumes for coexisting phases up to the critical temperature with a static method. *Fluid Ph. Equil.* 90, 177–187.
- Boedner, R.J., 1995. Fluid inclusion evidence for a magmatic source for metals in porphyry copper deposits. In: Thompson, J.F.H. (Ed.), *Magmas, Fluids and Ore Deposits*, Min. Assoc. Can. Short Course 23, pp. 139–152.
- Brugge, H., Hwang, C.-A., Rogers, W., Holste, J., Hall, K., Lemming, W., Esper, G., Marsh, K., Gammon, B., 1989. Experimental cross virial coefficients for binary mixtures of carbon dioxide with nitrogen, methane and ethane at 300 and 320 K. *Phys. A Stat. Mech. Appl.* 156 (1), 382–416.
- Cuney, M., Coulibaly, Y., Boiron, M.C., 2007. High-density early CO_2 fluids in the ultrahigh-temperature granulites of Ihouhoueuene (In Ouzzal, Algeria). *Lithos* 96 (3–4), 402–414.
- Davalos, J., Anderson, W.R., Phelps, R.E., Kidnay, A.J., 1976. Liquid-vapor equilibria at 250.00 K for systems containing methane, ethane, and carbon dioxide. *J. Chem. Eng. Data* 21 (1), 81–84.
- Davis, J.A., Rodewald, N., Kurata, F., 1962. Solid-liquid-vapor phase behavior of the methane-carbon dioxide system. *AIChE J.* 8 (4), 537–539.
- Deng, J., Liu, X., Wang, Q., Pan, R., 2015. Origin of the Jiadong-type Xinli gold deposit, Jiadong Peninsula, China: constraints from fluid inclusion and C–D–O–S–Sr isotope compositions. *Ore Geol. Rev.* 65 (Part 3), 674–686.
- Deng, J., Wang, Q., Li, G., Li, C., Wang, C., 2014a. Tethys tectonic evolution and its bearing on the distribution of important mineral deposits in the Sanjiang region, SW China. *Gondwana Res.* 26 (2), 419–437.
- Deng, J., Wang, Q., Li, G., Santosh, M., 2014b. Cenozoic tectono-magmatic and metallogenetic processes in the Sanjiang region, southwestern China. *Earth Sci. Rev.* 138, 268–299.
- Donnelly, H.G., Katz, D.L., 1954. Phase equilibria in the carbon dioxide–methane system. *Ind. Eng. Chem.* 46 (3), 511–517.
- Frey, M., Teichmüller, M., Teichmüller, R., Mullis, J., Kunzi, B., Breitschmid, A., Gruner, U., Schwizer, B., 1980. Very low-grade metamorphism in external parts of the Central Alps: illite crystallinity, coal rank and fluid inclusion data. *Eclog. Geol. Helv.* 73 (1), 173–203.
- Herskowitz, M., Kisch, H.J., 1984. An algorithm for finding composition, molar volume and isochores of CO_2-CH_4 fluid inclusions from Th and Tfm (for $\text{Th} < \text{Tfm}$). *Geochim. Cosmochim. Acta* 48 (8), 1581–1587.
- Heyen, G., Ramboz, C., Dubessy, J., 1982. Simulation of fluid phase-equilibria in the CO_2-CH_4 system below 50 °C and 100 bar: application to fluid inclusions. *C. R. De. L Acad. Des. Sci. Ser. II* 294 (3), 203–206.
- Hwang, S.-C., Lin, H.-M., Chapplear, P.S., Kobayashi, R., 1976. Dew point study in the vapor-liquid region of the methane-carbon dioxide system. *J. Chem. Eng. Data* 21 (4), 493–497.
- Jager, A., Span, R., 2012. Equation of state for solid carbon dioxide based on the Gibbs free energy. *J. Chem. Eng. Data* 57 (2), 590–597.
- Joffe, J., 1976. Vapor-liquid equilibria by the pseudocritical method. *Ind. Eng. Chem. Fundam.* 15 (4), 298–303.
- Lee, B.I., Kesler, M.G., 1975. A generalized thermodynamic correlation based on three-parameter corresponding states. *AIChE J.* 21, 510–527.
- Lemmon, E.W., Jacobsen, R.T., 1999. A generalized model for the thermodynamic properties of mixtures. *Int. J. Thermophys.* 20 (1), 825–835.
- Liu, D.H., Dai, J.X., Xiao, X.X., Tian, H., Yang, C., Hu, A.P., Mi, J.K., Song, Z.G., 2009. High density methane inclusions in Puguang Gasfield: discovery and a T-P genetic study. *Chin. Sci. Bull.* 54 (24), 4714–4723.
- Magee, J., Ely, J., 1988. Isochoric (p, v, T) measurements on CO_2 and (0.98 $\text{CO}_2 + 0.02 \text{CH}_4$) from 225 to 400 K and pressures to 35 MPa. *Int. J. Thermophys.* 9 (4), 547–557.
- Mao, S., Deng, J., Lü, M., 2015. A Helmholtz free energy equation of state for the $\text{NH}_3-\text{H}_2\text{O}$ fluid mixture: correlation of the PVTx and vapor–liquid phase equilibrium properties. *Fluid Ph. Equil.* 393, 26–32.
- Michelsen, M.L., 1993. Phase equilibrium calculations. What is easy and what is difficult? *Comput. Chem. Eng.* 17 (5–6), 431–439.
- Mondejar, M.a.E., Fernandez-Vicente, T.E., Haloua, F.D.R., Chamorro, C.S.R., 2012. Experimental determination of (p, p, T) data for three mixtures of carbon dioxide with methane for the thermodynamic characterization of nonconventional energy gases. *J. Chem. Eng. Data* 57 (9), 2581–2588.
- Mraw, S.C., Hwang, S.-C., Kobayashi, R., 1978. Vapor-liquid equilibrium of the methane-carbon dioxide system at low temperatures. *J. Chem. Eng. Data* 23 (2), 135–139.
- Neumann, A., Walch, W., 1968. Dampf/Flüssigkeits-Gleichgewicht CO_2/CH_4 im Bereich tiefer Temperaturen und kleiner CO_2 -Molenbrüche. *Chem. Ing. Tech.* 40 (5), 241–244.
- Parry, W.T., Blamey, N.J.F., 2010. Fault fluid composition from fluid inclusion measurements, Laramide age Uinta thrust fault. *Utah. Chem. Geol.* 278 (1–2), 105–119.
- Roedder, E., 1984. Fluid inclusions. In: *Reviews in Mineralogy*, 12. Mineralogy Society of America, Washington.
- Roedder, E., Bodnar, R.J., 1997. Fluid inclusion studies of hydrothermal ore deposits. In: Barnes, H.L. (Ed.), *Geochemistry of Hydrothermal Ore Deposits*, third ed. Wiley & Sons Inc., New York, pp. 657–698.
- Seitz, J.C., Blencoe, J.G., 1996. Volumetric properties for $\{(1-x)\text{CO}_2+x\text{CH}_4\}$, $\{(1-x)\text{CO}_2+x\text{N}_2\}$, and $\{(1-x)\text{CH}_4+x\text{N}_2\}$ at the pressures (19.94, 29.94, 39.94, 59.93, 79.93, and 99.93) MPa and the temperature 673.15 K. *J. Chem. Thermodyn.* 28 (11), 1207–1213.
- Seitz, J.C., Blencoe, J.G., Bodnar, R.J., 1996. Volumetric properties for $\{(1-x)\text{CO}_2+x\text{CH}_4\}$, $\{(1-x)\text{CO}_2+x\text{N}_2\}$, and $\{(1-x)\text{CH}_4+x\text{N}_2\}$ at the pressures (9.94, 19.94, 29.94, 39.94, 59.93, 79.93, and 99.93) MPa and temperatures (323.15, 373.15, 473.15, and 573.15) K. *J. Chem. Thermodyn.* 28 (5), 521–538.
- Setzmann, U., Wagner, W., 1991. A new equation of state and tables of thermodynamic properties for methane covering the range from the melting line to 625 K at pressures up to 1000 MPa. *J. Phys. Chem. Ref. Data* 20 (6), 1061–1155.
- Soave, G., 1972. Equilibrium constants from a modified Redlich-Kwong equation of state. *Chem. Eng. Sci.* 27 (6), 1197–1203.
- Somait, F.A., Kidnay, A.J., 1978. Liquid-vapor equilibriums at 270.00 K for systems containing nitrogen, methane, and carbon dioxide. *J. Chem. Eng. Data* 23 (4), 301–305.
- Span, R., Wagner, W., 1996. A new equation of state for carbon dioxide covering the fluid region from the triple-point temperature to 1100 K at pressures up to 800 MPa. *J. Phys. Chem. Ref. Data* 25 (6), 1509–1596.
- Span, R., Wagner, W., 1997. On the extrapolation behavior of empirical equations of state. *Int. J. Thermophys.* 18 (6), 1415–1443.
- Thiery, R., Dubessy, J., 1996. Improved modelling of vapour-liquid equilibria up to the critical region. Application to the $\text{CO}_2-\text{CH}_4-\text{N}_2$ system. *Fluid Ph. Equil.* 121 (1–2), 111–123.
- Thiery, R., Vandenbergkerhof, A.M., Dubessy, J., 1994a. vX properties of CH_4-CO_2 and CO_2-N_2 fluid inclusions: modeling for $T < 31^\circ\text{C}$ and $P < 400$ bars. *Eur. J. Mineral.* 6 (6), 753–771.
- Thiery, R., Vidal, J., Dubessy, J., 1994b. Phase equilibria modelling applied to fluid inclusions: liquid-vapour equilibria and calculation of the molar volume in the $\text{CO}_2-\text{CH}_4-\text{N}_2$ system. *Geochim. Cosmochim. Acta* 58 (3), 1073–1082.
- Tong, J., Liu, Y., 1984. The experimental study and correlation of PVT relation of binary gas mixture of carbon dioxide–methane. *J. Eng. Thermophys.* 5 (2), 119–124.
- van den Kerkhof, A.M., 1990. Isochoric phase diagrams in the systems CO_2-CH_4 and CO_2-N_2 : application to fluid inclusions. *Geochim. Cosmochim. Acta* 54 (3), 621–629.
- Vrabec, J., Fischer, J., 1996. Vapor-liquid equilibria of binary mixtures containing methane, ethane, and carbon dioxide from molecular simulation. *Int. J. Thermophys.* 17 (4), 889–908.
- Wang, P.J., Hou, Q.J., Wang, K.Y., Chen, S.M., Cheng, R.H., Liu, W.Z., Li, Q.L., 2007. Discovery and significance of high CH_4 primary fluid inclusions in reservoir volcanic rocks of the Songliao Basin, NE China. *Acta Geol. Sin. Engl. Ed.* 81 (1), 113–120.
- Webster, L.A., Kidnay, A.J., 2001. Vapor-liquid equilibria for the methane-propane–carbon dioxide systems at 230 K and 270 K. *J. Chem. Eng. Data* 46 (3), 759–764.
- Wei, M.-S.W., Brown, T.S., Kidnay, A.J., Sloan, E.D., 1995. Vapor+ liquid equilibria for the ternary system methane+ethane+carbon dioxide at 230 K and its constituent binaries at temperatures from 207 to 270 K. *J. Chem. Eng. Data* 40 (4), 726–731.
- Xu, N., Dong, J., Wang, Y., Shi, J., 1992. High pressure vapor liquid equilibria at 293 K for systems containing nitrogen, methane and carbon dioxide. *Fluid Ph. Equil.* 81, 175–186.
- Yoo, B.C., Brown, P.E., White, N.C., 2011. Hydrothermal fluid characteristics and genesis of Cu quartz veins in the Hwanggangri metallogenetic district, Republic of Korea: mineralogy, fluid inclusion and stable isotope studies. *J. Geochem. Explor.* 110 (3), 245–259.